A&A 423, 235–239 (2004)
DOI: 10.1051/0004-6361:20040161

Astronomy & Astrophysics

Research Note

Suggestions for an interstellar C_5H_2 search⋆

S. Chandra⋆⋆ and S. A. Shinde

School of Physical Sciences, SRTM University, Nanded 431 606, India
e-mail: sch@iucaa.ernet.in

Received 21 May 2003 / Accepted 5 May 2004

Abstract. Laboratory detection of four isomers of C_5H_2 molecule have been reported by Travers et al. (1997), McCarthy et al. (1997), and Gottlieb et al. (1998). They suggested for detection of the ring-chain isomer of C_5H_2 (c-C_5H_2) in cosmic objects, as it is the most stable one in comparison to the others. Two transitions 3_{13}–2_{12} and 3_{03}–2_{02} at 19.147 GHz and 19.606 GHz, respectively, of c-C_5H_2 have been detected in TMC-1. We suggest that the c-C_5H_2 may be identified in cool cosmic objects through its transition 3_{13}–4_{04} at 4.3 GHz in absorption against the cosmic microwave background. Since in absence of availability of the collisional rates, we have used scaled values for them, we have checked the sensitivity of the lines on the rates by enhancing the rate for the transitions with $\Delta k_a = 0$ by a factor of 10. Though the transitions are not found sensitive, our results may be treated as qualitative in nature. This absorption line may play an important role for identification of c-C_5H_2 in cosmic objects.

Key words. ISM: molecules

1. Introduction

After detection of C_4H_2 and C_6H_2 molecules in the expanding shell of the evolved carbon star IRC +10216 and in the rich-molecular-source TMC-1, search for C_5H_2 molecule in cosmic objects is being carried out. Out of the four isomers of C_5H_2 molecule, detected in laboratory by Travers et al. (1997), McCarthy et al. (1997), and Gottlieb et al. (1998), the ring-chain isomer (c-C_5H_2) is the most probable candidate for its detection in cosmic objects, as it is the most stable one as compared to the others. This isomer is an asymmetric top, planar molecule having. a large electric dipole moment $\mu = 3.5$ Debye inclined with the axes of inertia so that its components along the a and b axes of inertia are $\mu_a = 2.04$ Debye and $\mu_b = 2.89$ Debye. Thus, this isomer has both a-type and b-type radiative transitions, and therefore, the rotational energy levels cannot be separated into two different groups, as in case of an a-type or b-type molecule. Hence, the investigation of this molecule is quite complicated. The molecular data derived by Travers et al. (1997) for c-C_5H_2 are given in Table 1. Since the kinetic temperature in dark molecular clouds is rather low, only rotational transitions in the ground electronic and ground vibrational states take place. We propose to identify C_5H_2 in cosmic objects through its transition 3_{13}–4_{04} in absorption against the cosmic 2.73 K background (also called the cosmic microwave background, denoted as CMB).

Table 1. Molecular data.

A (MHz)	34 638.7013
B (MHz)	3424.87684
C (MHz)	3113.63865
Δ_J (MHz)	2.888×10^{-4}
Δ_{JK} (MHz)	2.952×10^{-2}
μ_a (Debye)	2.04
μ_b (Debye)	2.89

2. Einstein *A*-coefficients

Rotational wave functions for an asymmetric top molecule can be described by linear combination of symmetric top wave functions (Chandra et al. 1984a,b)

$$\Psi_{J\tau M}(\alpha,\beta,\gamma) = \sqrt{\frac{2J+1}{8\pi^2}} \sum_{K=-J}^{J} g^J_{\tau K} D^J_{MK}(\alpha,\beta,\gamma)$$

where α, β, γ are Euler angles specifying the orientation of the molecule, J the rotational quantum number, $g^J_{\tau K}$ the expansion coefficients, D^J_{MK} the Wigner D-function and the pseudo quantum number τ is defined by

$$\tau = k_a - k_c$$

⋆ Tables 3 is only available in electronic form at the CDS via anonymous ftp to cdsarc.u-strasbg.fr (130.79.128.5) or via http://cdsweb.u-strasbg.fr/cgi-bin/qcat?J/A+A/423/235

⋆⋆ Visiting Associate of IUCAA, Pune 411 007, India.

Article published by EDP Sciences and available at http://www.aanda.org or http://dx.doi.org/10.1051/0004-6361:20040161

Table 2. Energy levels of ring-chain isomer of C_5H_2.

J	k_a	k_c	E (cm^{-1})	J	k_a	k_c	E (cm^{-1})
0	0	0	0.000	1	0	1	0.218
2	0	2	0.654	1	1	1	1.259
1	1	0	1.270	3	0	3	1.308
2	1	2	1.685	2	1	1	1.716
4	0	4	2.180	3	1	3	2.324
3	1	2	2.386	4	1	4	3.175
5	0	5	3.269	4	1	3	3.279
5	1	5	4.239	5	1	4	4.395
6	0	6	4.575	2	2	1	4.840
2	2	0	4.840	3	2	2	5.494
3	2	1	5.494	6	1	6	5.516
6	1	5	5.734	7	0	7	6.097
4	2	3	6.366	4	2	2	6.366
7	1	7	7.006	7	1	6	7.296
5	2	4	7.457	5	2	3	7.457
8	0	8	7.835	8	1	8	8.707
6	2	5	8.765	6	2	4	8.765
8	1	7	9.081	9	0	9	9.789
7	2	6	10.291	7	2	5	10.301
9	1	9	10.621	3	3	1	10.726
3	3	0	10.726	9	1	8	11.088
4	3	2	11.598	4	3	1	11.598
10	0	10	11.958	8	2	7	12.035
8	2	6	12.051	5	3	3	12.689
5	3	2	12.689	10	1	10	12.747
10	1	9	13.318	9	2	8	13.996
6	3	4	13.998	6	3	3	13.998
9	2	7	14.021	11	0	11	14.340
11	1	11	15.086	7	3	5	15.525
7	3	4	15.525	11	1	10	15.770
10	2	9	16.175	10	2	8	16.213
8	3	6	17.271	8	3	5	17.271

where k_a and k_c are projections of J on the axis of symmetry in case of prolate and oblate symmetric tops, respectively. Rotational levels in an asymmetric top molecule are specified as J_{k_a,k_c} or J_τ. The rotational energy levels accounted in the present investigation are given in Table 2.

Since the electric dipole moment of the molecule is inclined with its axes of inertia, it has both a-type as well as b-type rotational transitions. The a-type rotational transitions are governed by the selection rules

J: $\Delta J = 0, \pm 1$

k_a, k_c: even, odd $\longleftrightarrow$ even, even

odd, even $\longleftrightarrow$ odd, odd.

In the representation where the axis of quantization is along the a-axis of inertia, Einstein A-coefficient for the transition $J'_{\tau'} \to J_\tau$ is (Chandra & Sahu 1993; Chandra & Rashmi 1998)

$$A\,(J'_{\tau'} \to J_\tau) = \frac{64\pi^4\nu^3\mu_a^2(2J+1)}{3hc^3(2J'+1)}\left[\sum_{K=-J}^{J} g^J_{\tau K} g^{J'}_{\tau' K} C^{J'K}_{JK10}\right]^2$$

where μ_a is the electric dipole moment along the a-axis of inertia, and $C^{\cdot\cdot}_{\cdots}$ the Clebsch Gordon coefficient. The b-type rotational transitions are governed by the selection rules

J: $\Delta J = 0, \pm 1$

k_a, k_c: even, odd $\longleftrightarrow$ odd, even

even, even $\longleftrightarrow$ odd, odd.

In the representation where the axis of quantization is along the a-axis of inertia, Einstein A-coefficient for the transition $J'_{\tau'} \to J_\tau$ is (Chandra et al. 1984b; Chandra 2002)

$$A\,(J'_{\tau'} \to J_\tau) = \frac{32\pi^4\nu^3\mu_b^2(2J+1)}{3hc^3(2J'+1)}\left[\sum_{K=-J}^{J} g^J_{\tau K}\Big(g^{J'}_{\tau' K+1} C^{J'K+1}_{JK11} + g^{J'}_{\tau' K-1} C^{J'K-1}_{JK1,-1}\Big)\right]^2$$

where μ_b is the electric dipole moment along the b-axis of inertia. Calculated values of Einstein A-coefficients for a-type as well as b-type rotational transitions between the levels up to 18 cm^{-1} are available in the electronic form in Table 3.

3. Collisional rate coefficients

Besides the radiative transition probabilities for optically allowed transitions between the rotational energy levels, data required as input for the present investigation are the rate coefficients for collisional transitions between the levels due to collisions with H_2 molecules. Though the collisional transitions are not restricted through any selection rules, computation of them is quite cumbersome task. The required collisional rate coefficients are not available in the literature. In absence of them qualitative investigations can however be carried out by choosing some scaling for the rate coefficients which do not favour any anomalous behaviour from their own. As and when the collisional rate coefficients would be available, the investigation can be repeated for quantitative results. In the present investigation, the rate coefficients for downward transitions $J'k'_ak'_c \to Jk_ak_c$ at a kinetic temperature T are taken as (Sharma & Chandra 2001)

$$C\,(J'k'_ak'_c \to Jk_ak_c) = 1 \times 10^{-11}\,\sqrt{T/30}/\,(2J'+1)\,.$$

These rate coefficients can be interpreted as the cross section times a thermal velocity. The factor $(2J'+1)$ is the degeneracy of the upper level of the transition. These rates have no selectivity and do not support any anomalous behaviour from their own. However, some transitions between the low lying levels may be sensitive to the collisional rates.

In order to investigate sensitivity of our results to the collisional rates, we enhanced the collisional rates for the transitions with $\Delta k_a = 0$ by a factor of 10 (i.e., by one order of magnitude), which may be taken as an extreme case. The results with these enhanced rates are also given in this paper. Moreover, in absence of accurate collisional rates, our results can be treated as qualitative in nature.

For upward collisional rate coefficients, we accounted for the fact that downward and upward collisional rate coefficients are related through the detailed equilibrium (Chandra & Kegel 2000).

4. Basic formulation

In our investigation, NLTE occupation numbers of the energy levels of the molecule under investigation are calculated in an on-the-spot approximation by using the escape probability method (see, e.g., Rausch et al. 1996), where the external radiation field, impinging on a volume element generating the lines, is the CMB only. Besides the normal features, some lines of a molecule may show anomalous features: (i) absorption against the CMB (called, anomalous absorption) and (ii) maser action.

4.1. Anomalous absorption

Observation of a spectral line in absorption against the CMB is an unusual phenomenon. The transition $1_{10} \rightarrow 1_{11}$ of H_2CO and $2_{20} \rightarrow 2_{11}$ of C_3H_2 are good examples of anomalous absorption. The intensity, I_ν, of a line generated in an interstellar cloud, with homogeneous excitation conditions, is given by

$$I_\nu - I_{\nu,\mathrm{bg}} = (S_\nu - I_{\nu,\mathrm{bg}})(1 - \mathrm{e}^{-\tau_\nu}) \qquad (1)$$

where $I_{\nu,\mathrm{bg}}$ is the intensity of the continuum against which the line is observed, τ_ν the optical depth of the line, and S_ν the source function. For positive optical depth, observation of an interstellar line in absorption against the CMB (i.e., $I_\nu < I_{\nu,\mathrm{bg}}$), obviously, implies the excitation temperature T_{ex} of the line to be less than the CMB temperature T_{bg}, but positive ($0 < T_{\mathrm{ex}} < T_{\mathrm{bg}}$). It requires rather peculiar conditions in the molecule generating the line. Equation (1) may also be expressed as

$$B_\nu(T_\mathrm{B}) - B_\nu(T_\mathrm{bg}) = \left[B_\nu(T_\mathrm{ex}) - B_\nu(T_\mathrm{bg})\right](1 - \mathrm{e}^{-\tau_\nu}) \qquad (2)$$

where B_ν represents a Planck's function corresponding to various temperatures and T_B is the brightness temperature of the line. (For absorption against the CMB, we have $T_\mathrm{B} < T_\mathrm{bg}$.) This obviously shows that for optically thin case, $\tau_\nu \approx 0$ and we have $T_\mathrm{B} = T_\mathrm{bg} \equiv 2.7$ K. Further, in the Rayleigh-Jeans limit [$\nu(\mathrm{GHz}) \ll 21\, T(\mathrm{K})$], Eq. (2) can be written as

$$T_\mathrm{B} = T_\mathrm{ex} + (T_\mathrm{bg} - T_\mathrm{ex})\mathrm{e}^{-\tau_\nu}. \qquad (3)$$

For anomalous absorption, we have $T_\mathrm{ex} < T_\mathrm{bg}$ and $\tau_\nu > 0$, and therefore, $T_\mathrm{B} > T_\mathrm{ex}$. When τ_ν is very large, then for the anomalous absorption, we have $T_\mathrm{B} = T_\mathrm{ex}$. It shows that for anomalous absorption, the brightness temperature of the line lies between T_ex of the line and T_bg ($T_\mathrm{ex} \le T_\mathrm{B} \le T_\mathrm{bg}$).

4.2. Maser action

Maser action is another anomalous phenomenon shown by some molecules in the cosmic objects. The molecules OH, H_2O and SiO are good examples of masing molecules. We can rearrange the Eq. (3) as

$$T_\mathrm{B} = T_\mathrm{bg}\mathrm{e}^{-\tau_\nu} - T_\mathrm{ex}(\mathrm{e}^{-\tau_\nu} - 1).$$

For maser action, we have population inversion and thus $T_\mathrm{ex} < 0$ and $\tau_\nu < 0$, showing that $T_\mathrm{B} > T_\mathrm{bg}$. When $|\tau_\nu|$ is large (such that $\mathrm{e}^{-\tau_\nu} \gg 1$), then for the maser action, we have

$$T_\mathrm{B} = (T_\mathrm{bg} - T_\mathrm{ex})\mathrm{e}^{-\tau_\nu}.$$

5. Numerical results and discussion

In our model, the free parametres are the hydrogen density n_{H_2} and $\gamma \equiv n_\mathrm{mol}/(\mathrm{d}v_r/\mathrm{d}r)$, where n_mol is density of the molecule, and $\mathrm{d}v_r/\mathrm{d}r$ the velocity gradient in the object. In order to include a large number of cosmic objects where c-C_5H_2 may be found, numerical calculations are carried out for wide ranges of physical parametres. We have taken two values 10^{-5} and 10^{-4} cm^{-3} (km s^{-1})$^{-1}$ pc for γ. For each value of γ, the molecular hydrogen density n_{H_2} is varied over the range from 10^3 to 10^6 cm^{-3}, and calculations are performed for two kinetic temperatures 10 and 20 K, as the temperature in the clouds cannot be larger than this. In the present investigation, a set of 64 linear equations coupled with 274 equations of radiative transfer is solved through the iterative procedure for given values of n_{H_2} and γ.

5.1. Observations

For the observed two transitions 3_{13}–2_{12} and 3_{03}–2_{02} at 19.147 GHz and 19.606 GHz, respectively of c-C_5H_2 detected in TMC-1, Dickens et al. (2001) obtained $\Delta v = 0.15$ km s^{-1}, and the upper limits for the relative column density of c-C_5H_2 was obtained as 2×10^{12} cm^{-2} and 4×10^{12} cm^{-2}, respectively. (Frequencies of these transitions given in Table 1 of Dickens et al. (2001) suffer from misprint as we discussed with them.) For these values of Dickens et al. (2001), the corresponding values of the free parametre γ are 4.5×10^{-6} and 9×10^{-6} cm^{-3} (km s^{-1})$^{-1}$ pc. This higher value 9×10^{-6} is closed to our value 10^{-5}, and our second value is larger by one order of magnitude.

For the observed lines 3_{13}–2_{12} and 3_{03}–2_{02}, variation of brightness temperature T_B versus the hydrogen density n_{H_2} for $T = 10$ K (row 1) and 20 K (row 2) is shown in Fig. 1. We found $T_\mathrm{B} > T_\mathrm{bg}$, although not very large for $\gamma = 10^{-5}$, but showing emission feature for both the lines. Since both the lines are detected in emission, the reason for low value of ($T_\mathrm{B} - T_\mathrm{bg}$) in our calculations can be assigned to the qualitative nature of our investigations. When γ (i.e., $N(c\text{-}C_5H_2)/\Delta v$) is increased by one order of magnitude, T_B shows a remarkable increase where optical depth τ_ν goes up to 0.4 and 0.5 at $T = 10$ K, and 0.06 and -0.1 at $T = 20$ K for 3_{13}–2_{12} and 3_{03}–2_{02} transitions, respectively. The results with the enhanced collisional rates for the lines are shown in rows 3 and 4 of Fig. 1. With the enhanced rates, a little increase in T_B is found; which is more remarkable on the two sides of the peak. The peak in T_B is found to shift towards the low density region, and at the peak, the optical depth is found to decrease.

5.2. The 7_{07}–6_{16} and 6_{06}–5_{15} transitions

A number of lines of c-C_5H_2 were found showing negative value for the excitation temperature (maser action). Though it was not large in magnitude, we have however investigated two transitions 7_{07}–6_{16} and 6_{06}–5_{15} at 17.4 GHZ and 10.1 GHz, respectively. Other lines showing negative value for T_ex were insignificant. Variation of T_B versus n_{H_2} for these two lines is also shown in Fig. 1. The optical depth, at the peak, goes up

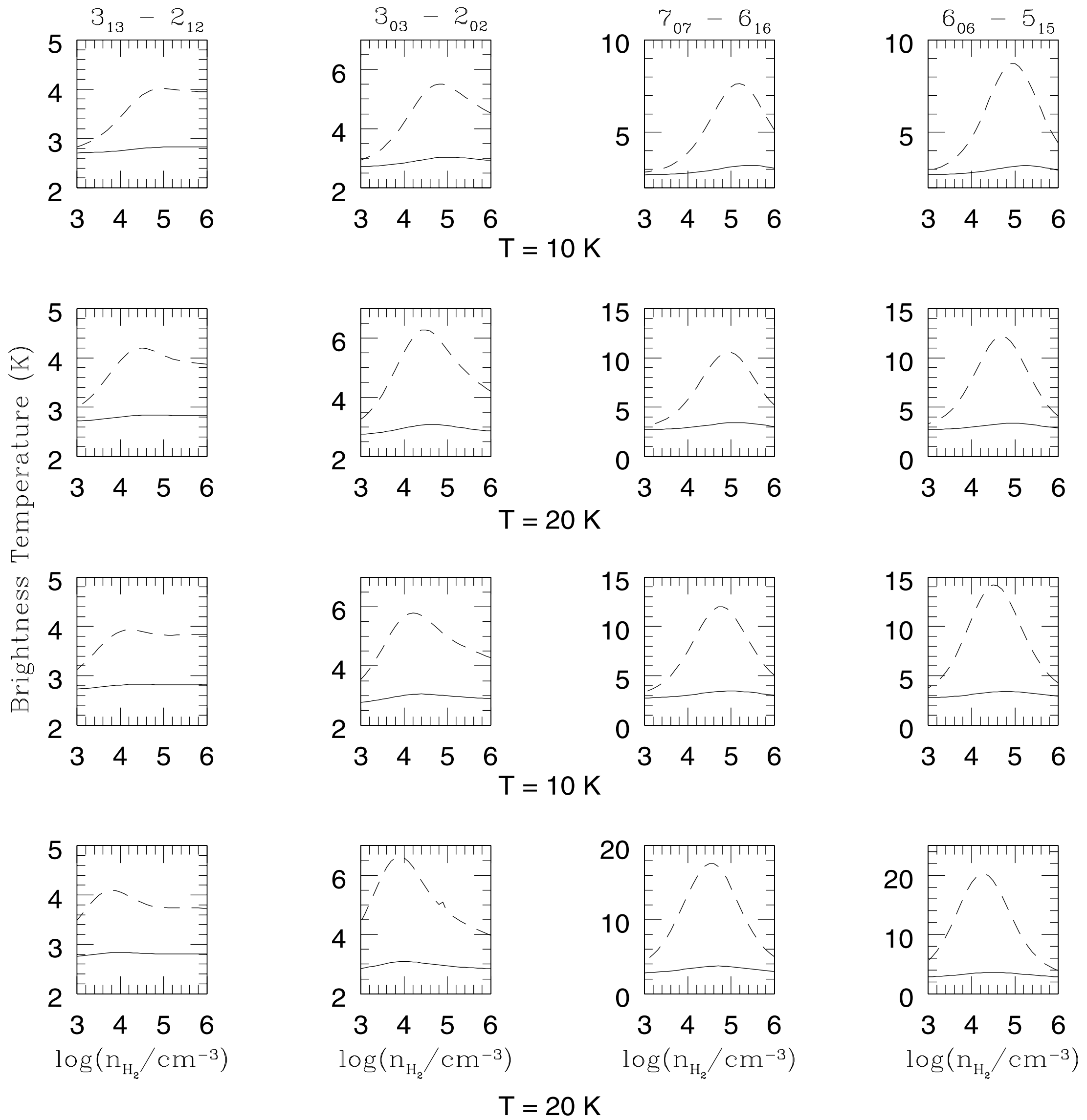

Fig. 1. Variation of brightness temperature T_B (K) versus hydrogen density n_{H_2} of the lines written at the top of each column for kinetic temperatures 10 K (rows 1 and 3) and 20 K (rows 2 and 4). Solid line is for $\gamma = 10^{-5}$ cm^{-3} (km s^{-1})$^{-1}$ pc, and the dotted line for $\gamma = 10^{-5}$ cm^{-4} (km s^{-1})$^{-1}$ pc. Lower rows (3 and 4) are for the case where collisional rates of the transitions with $\Delta k_a = 0$ are increased by a factor of 10.

to −0.5 and 0.2 at $T = 10$ K, and −0.8 and 0.1 at $T = 20$ K for 7_{07}−6_{16} and 6_{06}−5_{15}, respectively. The effect of the enhancement of collisional rates for these lines is found more prominent than those observed ones. With the enhanced collisional rates, at the peak, the optical depth goes up to −1.0 and 0.3 at $T = 10$ K, and −1.4 and 0.06 at $T = 20$ K for 7_{07}−6_{16} and 6_{06}−5_{15}, respectively.

5.3. The 3_{13}−4_{04} transition

A number of lines of c-C_5H_2 are found in absorption against the cosmic 2.7 K background. However, the transition 3_{13}−4_{04} at 4.3 GHz has shown reasonably good absorption phenomenon. Einstein A-coefficient for this transition is 1.74×10^{-9} s^{-1}. For this transition, we have plotted brightness temperature T_B (Col. 1), excitation temperature T_{ex} (Col. 2), optical depth τ_ν (Col. 3) and again T_B where the enhanced collisional rates are used (Col. 4). Anomalous absorption is found to increase with γ. A moderate increase is found with the increase of kinetic temperature T, where the position of the minimum value of T_B is found to shift towards the low density region.

It is interesting to have a note that the observed transition 3_{13}−2_{12} ($A = 1.30 \times 10^{-7}$ s^{-1}) is detected in emission whereas the transition 3_{13}−4_{04}, having the common upper level 3_{13} shows absorption against the CMB. The process of absorption can be understood in the following manner. The level 3_{13}, besides to 4_{04}, decays radiatively to the levels 2_{12} and 2_{02} ($A = 3.49 \times 10^{-6}$ s^{-1}). The lower level 4_{04} has only one radiative decay to 3_{03} ($A = 3.84 \times 10^{-7}$ s^{-1}). The radiative life time of the level 3_{13} (2.8×10^5 s) of the transition is one order of magnitude smaller than that of the level 4_{04} (2.6×10^6 s). Thus, the molecule in the lower level exists longer and can absorb the

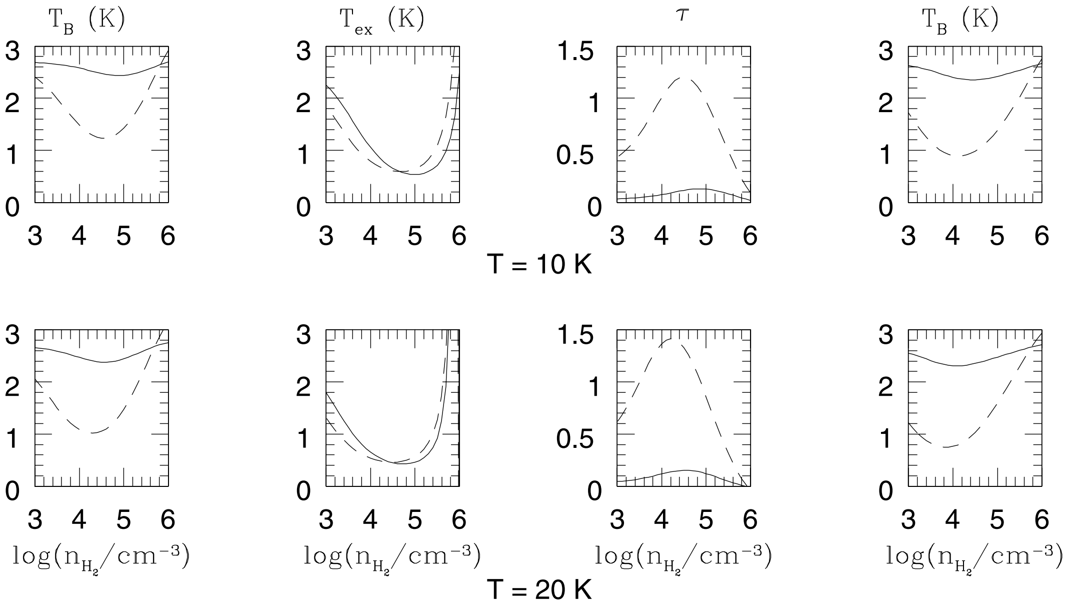

Fig. 2. Variation of brightness temperature T_{B} (Col. 1), excitation temperature T_{ex} (Col. 2), optical depth τ_ν (Col. 3) and brightness temperature with enhanced collisional rates (Col. 4) versus hydrogen density $n_{\mathrm{H_2}}$ of 3_{13}−4_{04} transition. Solid line is for $\gamma = 10^{-5}$ cm^{-3} (km s^{-1})$^{-1}$ pc, and the dotted line for $\gamma = 10^{-4}$ cm^{-3} (km s^{-1})$^{-1}$ pc. For the brightness temperature T_{B} in Col. 4, the collisional rates for the transitions with $\Delta k_a = 0$ are increased by a factor of 10.

radiations corresponding to the transition 3_{13}−4_{04} coming from the background.

6. Conclusion

Here, we have used scaled values of collisional rates, and therefore, our results are qualitative in nature. We have obtained emission feature of the observed lines qualitatively. We found that detection of c-C_5H_2 is likely in cool cosmic objects through anomalous absorption of the transition 3_{13}−4_{04}. In absence of accurate collisional rates, our investigation provides information that this transition may play important role for identification of c-C_5H_2 in cool cosmic objects.

Acknowledgements. We are grateful to Prof. Jayant V. Narlikar, Prof. Dr. W. H. Kegel and Prof. S. A. Suryawanshi for their encouragement. Thanks are due to learned referee for constructive and valuable comments which improved the manuscript a lot.

References

Chandra, S. 2002, Ind. J. Phys., 76B, 649
Chandra, S., & Kegel, W. H. 2000, A&AS, 142, 113
Chandra, S., & Rashmi 1998, A&AS, 131, 137
Chandra, S., & Sahu, A. 1993, A&A, 272, 700
Chandra, S., Kegel, W. H., & Varshalovich, D. A. 1984a, A&AS, 58, 687
Chandra, S., Varshalovich, D. A., & Kegel, W. H. 1984b, A&AS, 55, 51
Dickens, J. E., Langer, W. D., & Velusamy, T. 2001, ApJ, 558, 693
Gottlieb, C. A., McCarthy, M. C., Gordon, V. D., et al. 1998, ApJ, 509, L141
McCarthy, M. C., Travers, M. J., Kovacs, A., et al. 1997, Science, 275, 518
Rausch, E., Kegel, W. H., Tsuji, T., & Piehler, G. 1996, A&A, 315, 533
Sharma, A. K., & Chandra, S. 2001, A&A, 376, 333
Travers, M. J., McCarthy, M. C., Gottlieb, C. A., & Thaddeus, P. 1997, ApJ, 483, L135